PCCP

RSC Publishing

COMMUNICATION

View Article Online
View Journal | View Issue

Molecular direction dependence of single-molecule conductance of a helical peptide in molecular junction†

Cite this: *Phys. Chem. Chem. Phys.*, 2013, **15**, 757

Received 4th October 2012,
Accepted 16th November 2012

DOI: 10.1039/c2cp43499g

www.rsc.org/pccp

Hirotaka Uji, Tomoyuki Morita and Shunsaku Kimura*

Published on 30 November 2012 on http://pubs.rsc.org | doi:10.1039/C2CP43499G
Downloaded by Osaka University on 04 January 2013

The helix-peptide dipole effect on single-molecule conductance was analysed experimentally and theoretically with a single 8mer helical peptide. The helical peptide was immobilized on a gold surface in two opposite directions of the helix dipole. Single-molecule conductance of the helical peptide was determined to be 2.4 × 10^{-5} G_0 by scanning tunneling microscopy (STM) break-junction measurements under the condition of applied bias voltage parallel to the dipole, which was about 1.2-fold larger than that in the anti-parallel direction. Theoretical calculation also supports that the helix dipole influences the electron transport reaction depending on parallel or anti-parallel orientation of the dipole against the applied electric field.

Investigations on electric properties of a single organic molecule are essential for development in the field of molecular electronics, which utilizes molecules as modules of electrical devices. The concept of a single molecule rectifier was proposed by Aviram and Ratner in 1974.[1] To date, studies on electron transfer through a single organic molecule have been extensively carried out experimentally and theoretically. We have focused our attention on helical peptides because of their relatively high conductance over a long distance,[2–5] regular molecular shape,[6] and large dipole moment.[7–9]

Single-molecule electric properties of peptides have been investigated by mainly following two methods. One is scanning tunneling spectroscopy (STS), which provides current–voltage profiles to detect the bias-dependent property of molecular conductance.[10,11] The other is scanning tunneling microscopy (STM) break-junction measurement, which evaluates single-molecule conductance[12] with properties of distance decay.[13–15] STS has the drawback of the asymmetric configuration of the gap between the tip and one molecular terminal. On the other hand, the STM break-junction method has difficulty in immobilization of molecules between electrodes with a determined molecular orientation. These points still leave the discussions on the molecular rectification of helical peptides vague, especially concerning the effect of the molecular dipole on the molecular conductance.

In this work, we report electric properties of a single helical peptide analysed by the STM break-junction method with a symmetric configuration about the gold–peptide–gold junction but under defined molecular direction. The peptides synthesized here are 8mer helical peptides having an alternating

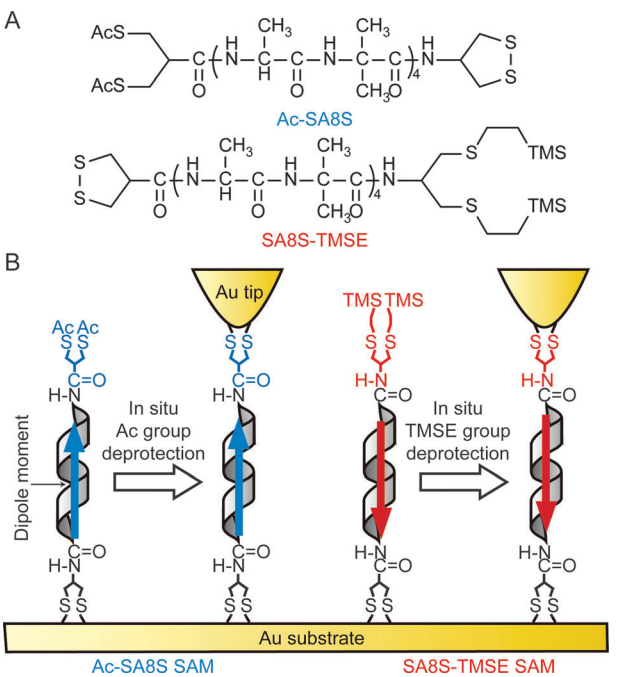

Fig. 1 (A) Chemical structures of the helical peptides and (B) schematic illustration of the STM break-junction measurements with the helical peptides immobilized on gold substrate.

Department of Material Chemistry, Graduate School of Engineering, Kyoto University, Kyoto-Daigaku-Katsura, Nishikyo-ku, Kyoto, 615-8510, Japan.
E-mail: shun@scl.kyoto-u.ac.jp; Fax: +81 75 383 2401; Tel: +81 75 383 2400

† Electronic supplementary information (ESI) available: Synthesis of helical peptides, circular dichroism spectroscopy, preparation of self-assembled monolayers, molecular modeling, IRRAS measurements, ellipsometry, cyclic voltammetry, STM measurements, and theoretical calculation. See DOI: 10.1039/c2cp43499g

Published on 30 November 2012 on http://pubs.rsc.org | doi:10.1039/C2CP43499G
Downloaded by Osaka University on 04 January 2013

sequence of Ala and α-aminoisobutyric acid (Aib) (Fig. 1A). Aspargusic acid or its amine analogue was introduced either at the N terminal or the C terminal, to immobilize the peptides *via* two Au–S linkages. Importantly, in both cases two carbon groups came to be inserted between the Au–S linkage and the adjacent peptide bond. The opposite ends of the peptides were connected with two thiol groups with suitable protecting groups. Again, these linker parts are also designed to be composed of two Au–S linkages, and two carbon groups intervening between the Au–S linkage and the adjacent peptide bond when these moieties are used to immobilize the peptides in the junction (Fig. 1A).

Therefore, the two protected thiol groups and the disulfide group were placed at the two terminals of the peptides.[16] The latter disulfide group was first used for immobilization of the peptides to gold substrates. Subsequently, the two thiol groups were deprotected to react with gold tips. With a series of these processes, the peptides were immobilized in the junction with a defined molecular orientation and a symmetric configuration, Au–(S–(CH_2))$_2$–CH–(peptide bond)–(8mer peptide)–(peptide bond)–CH–((CH_2)–S)$_2$–Au (Fig. 1B).

Detailed characterizations of the self-assembled monolayers (SAMs) of the peptides were carried out (ESI†). Using the infrared reflection–absorption spectroscopy (IRRAS), both peptides showed amide I absorption at around 1668 cm^{-1} and amide II absorption at around 1536 cm^{-1}, suggesting the peptides take a helical conformation on the gold substrate. Based on the absorbance ratios of amide I and amide II,[17] the tilt angles of the helix axis from the surface normal were calculated to be 60° for the Ac-SA8S SAM and 45° for the SA8S-TMSE SAM. The monolayer thicknesses estimated by ellipsometry were consistent with the values calculated using these tilt angles. The SA8S-TMSE SAM was confirmed to be densely packed by cyclic voltammetry in an aqueous $K_4[Fe(CN)_6]$ solution. On the other hand, the Ac-SA8S SAM was loosely packed, which is in agreement with the large tilt angle in the SAM. The negative dipole at the C terminal should destabilize formation of the Au–S linkage where the thiol atom bears a negative partial charge.[18]

The peptide monolayers were treated with a basic solution to remove protecting groups.[19] The gold STM tip was placed over a large terrace with the peptide monolayer and moved toward the monolayer surface to form a gold–peptide–gold junction. Approximately 10 000–20 000 current–distance curves were collected at a bias voltage of −0.1 V in toluene at several points on the sample. These curves were categorized into three types: curves of exponential distance decay corresponding to absence of molecules in the junction (Fig. 2A right and B right), noisy curves, and curves with step-like features which are proof of a gold–peptide–gold junction formation (Fig. 2A left and B left).[12,20] The tip position was transferred to another large terrace after data collections of about every 500 curves to avoid influence of the thermal drift of the tip. The ratios of these three types were about 60 : 30 : 10 for Ac-SA8S and 70 : 25 : 5 for SA8S-TMSE, showing that the curves of exponential distance decay were mainly recorded.

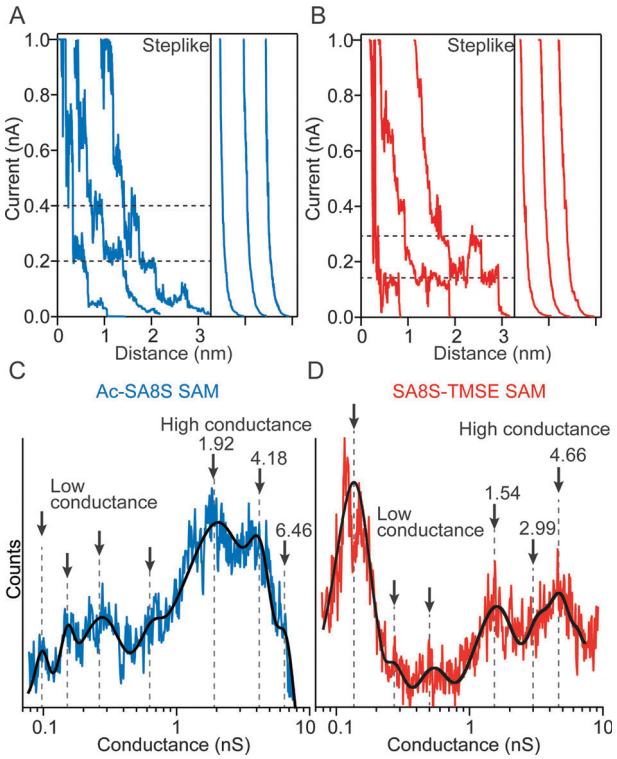

Fig. 2 (A, B) Current–distance curves and (C, D) conductance histograms of peptides: (A, C) Ac-SA8S; (B, D) SA8S-TMSE.

The conductance histograms based on the approximately 1000 current–distance curves with step-like features are shown in Fig. 2C and D. The histograms can be divided into two regions of high and low conductance using 1 nS as a boundary value. The peaks in the low conductance region are generally attributed to different contact geometries about gold–sulfur linkages. On the other hand, three peaks at 1.92, 4.18, and 6.46 nS in the high conductance region of Ac-SA8S are assigned to conductance of one, two, and three molecules in a junction, respectively (Fig. 2C). A single molecule conductance of Ac-SA8S is therefore determined to be 1.92 nS (2.4×10^{-5} G_0, where $G_0 = 2e^2/h$ (e is the electron charge and h the Planck constant)). Similarly, the histogram for SA8S-TMSE shows integral multiple peaks at 1.54, 2.99, and 4.66 nS in the high conductance region, indicating single molecule conductance of 1.54 nS (2.0×10^{-5} G_0) for SA8S-TMSE (Fig. 2D). Either conductance is far larger than that of octadecanedithiol having a similar molecular length (2.5 nm) at 4.0×10^{-9} G_0 (calculated using the data in the literature[12,21]), but about 5-fold smaller than the 3mer of oligo(*p*-phenylene ethynylene) dithiol of 1.3×10^{-4} G_0.[22] These relatively high conductances of the helical peptides are consistent with the previous report on the distance decay constant of electron transfer rate along helical peptides of 0.32 Å^{-1}.[23]

Single-molecule conductance of Ac-SA8S is about 1.25-fold larger than that of SA8S-TMSE. These conductances were obtained with the negative bias where electrons flow from substrates to tips. This flow direction coincides with the dipole direction of Ac-SA8S and opposes to that of SA8S-TMSE. Ac-SA8S and SA8S-TMSE are designed to have the same

 This journal is © the Owner Societies 2013

Published on 30 November 2012 on http://pubs.rsc.org | doi:10.1039/C2CP43499G
Downloaded by Osaka University on 04 January 2013

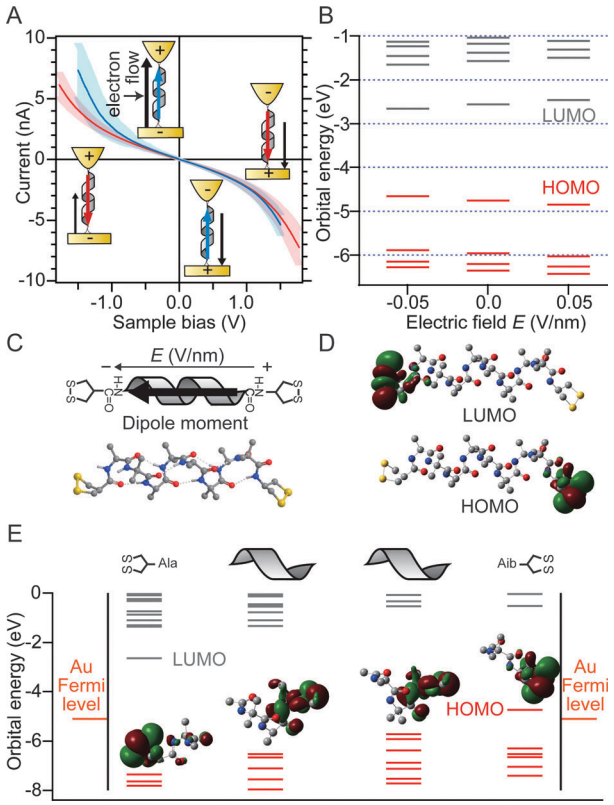

Fig. 3 (A) Current–voltage (*I–V*) curves of SAMs: (blue) Ac-SA8S; (red) SA8S-TMES. (B) Molecular orbital energy spectra of SA8S applying voltages at the C terminal and taking the N terminal as zero. (C) The energy-minimized conformation of the peptide (bottom) and directions of the helix dipole and the positive electric field applied to the peptide. (D) Frontier molecular orbitals of SA8S at zero bias. (E) Molecular fragmentation energy diagrams in the molecular junction.

molecular structure after formation of the gold–peptide–gold junction, as described before. The different conductance between the two peptides are therefore considered as a result of the dipole effect of the helical peptides on the electron flow.

Current–voltage (*I–V*) profiles of the two peptides were obtained as average curves with the standard deviations based on 500 *I–V* curves of each peptide (Fig. 3A). Weak rectification behavior was observed with rectification ratios, $R = |I(1.5)/I(-1.5)|$, of 0.76 and 1.2 for Ac-SA8S and SA8S-TMSE, respectively. These values agree well with the single-molecule conductance difference between the two peptides by STM break-junction measurements, showing that the electron flow along the dipole direction of the helical peptides is facilitated by about 20%. When the *I–V* curve of Ac-SA8S is compared with that of SA8S-TMSE in Fig. 3A, the current through SA8S-TMSE with the positive bias was weaker than that through Ac-SA8S, which appears opposite to the dipole effect on the conductance described above. However, this result is explainable by the fact that monolayer thickness of Ac-SA8S is thinner than that of SA8S-TMSE (Table S1, ESI†). Previously, our study of redox-active functionalized peptides showed that the electron transfer in a helical peptide monolayer depended on the tilt angle of the peptides.[23] The tilted orientation shortened the direct distance for electron transfer. Further, an intermolecular electron transfer process *via* a few peptide molecules might be involved. In these STS measurements, the tip was kept at the same position on the monolayer, which was determined by the initial set current, whereas in the STM break-junction measurements the tip lifted up molecules. These factors should explain the larger current of Ac-SA8S than SA8S-TMSE. Therefore, the data in Fig. 3A should be examined with each molecule and not between the two.

The two complementary experiments consistently show that the helix dipole accelerates electron flow along the dipole direction by about 20% that in the reversed arrangement of the dipole and the electron flow. The degree of a few tens percent is very low compared with those reported values of about 3-fold acceleration along the helical peptides in solution[24] and on gold substrate.[25] There may be several factors to explain the differences in the acceleration effects of dipoles between these experimental results, for example whether the peptides were in solution or on gold. However, the method adopted here is the most reliable for the evaluation of single-molecule conductance, because the data were obtained strictly with a single molecule under the defined molecular orientation in the junction.

First-principle calculations were carried out to get more insight of the external electric-field effect on orbital energies. Fig. 3B shows changes of molecular orbitals energies under applying bias voltage. When the electric field is applied to the peptide molecule antiparallel to the dipole, the HOMO level moves up and the LUMO level moves down (Fig. 3B, left). These changes are easily explained by the localization of the HOMO state at the C terminal and of the LUMO state at the N terminal due to the dipole (Fig. 3D). The applied electric field from the N terminal to the C terminal therefore destabilizes the HOMO state to raise the orbital energy level. On the other hand, with this electric field, the LUMO state lowers the orbital energy level. In the case of the electric field applied parallel to the dipole, the situation is reversed to widen the energy gap between the HOMO state and the LUMO state (Fig. 3B, right). Since the Fermi level of Au electrode is close to the HOMO orbital energy level, electrons are considered to tunnel *via* virtually using the HOMO orbital. The electronic coupling between the Au electrode and the HOMO orbital localized at the C terminal therefore becomes strong with the electric field applied antiparallel to the dipole, which can explain the rectification property of the peptides observed here.[26]

The electron transfer distance is over 2 nm with the peptides, meaning that the HOMO orbitals of the intervening amide bonds should also contribute to the electron tunneling. To know the energy diagrams including the peptide moieties, the peptide is divided into four parts of linker-Ala, two tripeptides, and Aib-linker, as shown in Fig. 3E. Molecular conformations of the four parts were taken to be the energy-minimized conformation of the whole peptide calculated at zero bias voltage (Fig. 3C), and the molecular orbitals of the four parts were calculated by single point calculation. With a negative bias voltage applied to the C terminal, the Au Fermi level of the right electrode in Fig. 3E moves up and that of the left one moves down. On the other hand,

the HOMO orbital energy levels move up under the electric field applied antiparallel to the dipole (Fig. 3B left). The energy diagram was compared with that from applying the opposite bias voltage, and the electron coupling of the right Au electrode with the HOMO orbitals of the four parts was evaluated (Fig. S4, ESI†). Available HOMO orbitals between the two Fermi levels for electron tunneling are larger with a negative bias voltage applied to the C terminal than with a positive bias voltage, which can explain consistently the present observations that helix dipole affects electron transfer.

In summary, we have determined the single-molecule conductance of 8mer helical peptides by the STM break-junction measurements. Conductance of the helical peptide depends on the electron flow direction from N terminal to C terminal or from C terminal to N terminal due to the intrinsic dipole moment along the helix. The electron flow along the dipole moment was about 1.2-fold larger than the opposite direction. Theoretical studies qualitatively explain the asymmetric molecular conductance on the electron flow direction with respect to the dipole direction.

Published on 30 November 2012 on http://pubs.rsc.org | doi:10.1039/C2CP43499G
Downloaded by Osaka University on 04 January 2013

Acknowledgements

This work was financially supported partially by Grant-in-Aid for Scientific Research B (21350061), JSPS Fellows (24 5908). H.U. acknowledges the Research Fellowships of the Japan Society for the Promotion of Science for Young Scientists.

Notes and references

1 A. Aviram and M. A. Ratner, *Chem. Phys. Lett.*, 1974, **29**, 277–283.
2 Y. Arikuma, H. Nakayama, T. Morita and S. Kimura, *Angew. Chem., Int. Ed.*, 2010, **49**, 1800–1804.
3 M. Sisido, S. Hoshino, H. Kusano, M. Kuragaki, M. Makino, H. Sasaki, T. A. Smith and K. P. Ghiggino, *J. Phys. Chem. B*, 2001, **105**, 10407–10415.
4 S. Antonello, F. Formaggio, A. Moretto, C. Toniolo and F. Maran, *J. Am. Chem. Soc.*, 2003, **125**, 2874–2875.
5 T. Morita and S. Kimura, *J. Am. Chem. Soc.*, 2003, **125**, 8732–8733.
6 K. Otoda, Y. Kitagawa, S. Kimura and Y. Imanishi, *Biopolymers*, 1993, **33**, 1337–1345.
7 S. Kimura, *Org. Biomol. Chem.*, 2008, **6**, 1143–1148.
8 J. Watanabe, T. Morita and S. Kimura, *J. Phys. Chem. B*, 2005, **109**, 14416–14425.
9 D. Cristancho and J. M. Seminario, *J. Chem. Phys.*, 2010, **132**, 065102.
10 K. Kitagawa, T. Morita and S. Kimura, *Angew. Chem., Int. Ed.*, 2005, **44**, 6330–6333.
11 K. Kitagawa, T. Morita and S. Kimura, *J. Phys. Chem. B*, 2005, **109**, 13906–13911.
12 B. Xu and N. J. Tao, *Science*, 2003, **301**, 1221–1223.
13 X. Xiao, B. Xu and N. J. Tao, *J. Am. Chem. Soc.*, 2004, **126**, 5370–5371.
14 S. Sek, A. Misicka, K. Swiatek and E. Maicka, *J. Phys. Chem. B*, 2006, **110**, 19671–19677.
15 L. Scullion, T. Doneux, L. Bouffier, D. G. Fernig, S. J. Higgins, D. Bethell and R. J. Nichols, *J. Phys. Chem. C*, 2011, **115**, 8361–8368.
16 I. Díez-Pérez, J. Hihath, Y. Lee, L. Yu, L. Adamska, M. A. Kozhushner, I. I. Oleynik and N. J. Tao, *Nat. Chem.*, 2009, **1**, 635–641.
17 R. Schwyzer, P. Moutevelis-Minakakis, S. Kimura and H. Gremlich, *J. Pept. Sci.*, 1997, **3**, 65–81.
18 S. Yasutomi, T. Morita, Y. Imanishi and S. Kimura, *Science*, 2004, **304**, 1944–1947.
19 G. M. Morales, P. Jiang, S. Yuan, Y. Lee, A. Sanchez, W. You and L. Yu, *J. Am. Chem. Soc.*, 2005, **127**, 10456–10457.
20 T. Morita and S. Lindsay, *J. Phys. Chem. B*, 2008, **112**, 10563–10572.
21 F. Chen, X. Li, J. Hihath, Z. Huang and N. J. Tao, *J. Am. Chem. Soc.*, 2006, **128**, 15874–15881.
22 Q. Lu, K. Liu, H. Zhang, Z. Du, X. Wang and F. Wang, *ACS Nano*, 2009, **3**, 3861–3868.
23 K. Takeda, T. Morita and S. Kimura, *J. Phys. Chem. B*, 2008, **112**, 12840–12850.
24 E. Galoppini and M. A. Fox, *J. Am. Chem. Soc.*, 1996, **118**, 2299–2300.
25 T. Morita, S. Kimura, S. Kobayashi and Y. Imanishi, *J. Am. Chem. Soc.*, 2000, **122**, 2850–2859.
26 J. B. Pan, Z. H. Zhang, X. Q. Deng, M. Qiu and C. Guo, *Appl. Phys. Lett.*, 2011, **98**, 013503.

 This journal is © the Owner Societies 2013